In Vitro Assembly of Bacteriophage λ Procapsids for use as Viral Nanoparticles

Katie Biscocho*

Under the mentorship of Dr. Arianne Jansma and Dr. Kristopher Koudelka*, with committee member Nicole Jones*****

* Department of Biology, Point Loma Nazarene University
** Department of Chemistry, Point Loma Nazarene University
***Point Loma Nazarene University, Class of 2021

Bacteriophage λ procapsids as effective drug transporters provide promising means of patient care and treatment within the medical field with implications in targeted drug delivery. The 3D icosahedral shape is constituted primarily of two proteins: gpE and gpD. Another protein, gpNu3, acts as a scaffold that mediates capsid protein assembly. Isolation of and subsequent introduction of each protein into a drug containing solution provides the opportunity for encapsulation of therapeutic drugs to be enveloped in an editable, fully formed viral container *in vitro,* thus improving payload concentration. Protein production, identification and purification techniques utilizing glutathione-S-transferase (GST) tags and affinity columns were evaluated in order to isolate individual procapsid components for further assembly. The success of procapsid formation *in vitro* using various ratios of gpE:gpD:gpNu3 was also evaluated. SEC data indicates that the combination of GST-cleaved gpE, gpD, and gpNu3 formed aggregates that were smaller than fully formed procapsids. However, the manipulation of capsid protein ratios yielded different size exclusion chromatography (SEC) peak formations, suggesting that the decrease in gpNu3 concentration and the addition of gpD in direct proportion to gpE resulted in an increase in the uniformity of structure development, which is a promising step into controlled formation of procapsids *in vitro*.

λ

Introduction

Modern science has seen the increase in usage of nanoscale technology within the realm of medicine, driving the advancement of therapeutic solutions and medical diagnoses (De Jong *et al.* 2022). Common types of nanotechnology like organic liposome and lipid-based particles are currently capable of being manufactured with specified criteria, allowing for their utilization in targeted drug delivery and fluorescent imaging. However, problems arise when examining their upscale production, biocompatibility, and low stability amidst engineering (Anselmo *et al.* 2016).

Deriving nanoparticles from other sources, such as viruses, have implications in combatting these obstacles. They are known to replicate naturally on a large-scale, making upscale manufacturing of viral nanoparticles (VNPs) a viable option for the health economy. This is also paired with their natural function of host-infection through genome delivery, which improves their biocompatibility as effective molecular transporters. Lastly, greater structure stability due to a high-protein constitution in viral shells allows for further VNP chemical modulation that is otherwise too harsh for nanoparticles from other origins (Koudelka *et al.* 2015).

It is especially beneficial to derive VNPs from viruses with non-human hosts to increase the safety and efficacy of clinical nanoscale drug-delivery systems. One example is the extensively researched bacteriophage λ, which infects the bacterium *Escherichia coli* (*E. coli*). The full capsid head, or "procapsid", component of the virus is capable of production *in* vivo, and possesses the propensity to act as an efficient

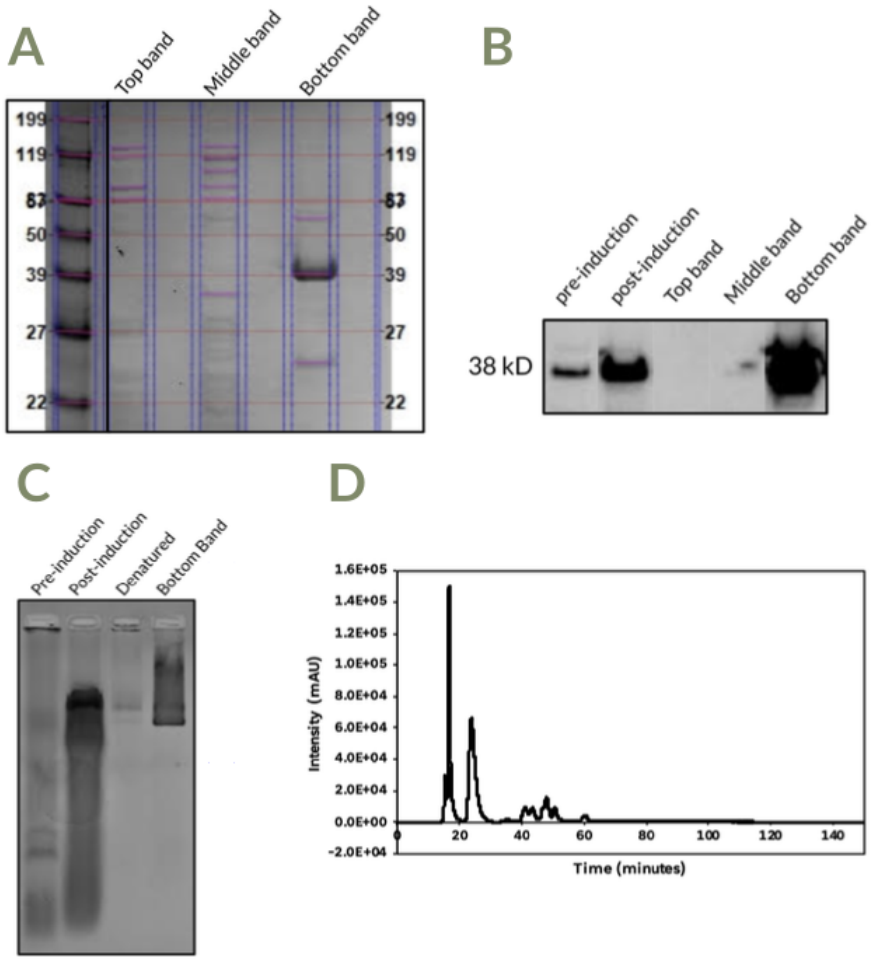

Figure 1. **Intact procapsids can be made *in vivo.*** (A) Sucrose gradient bands were analyzed using SDS-Page. Three bands resulted from the purification procedure and pulled for gel loading. (B) Sucrose gradient bands were also analyzed using western blotting. Chemiluminescent signals using Anti-gpE antibodies were examined to visualize the presence of gpE. (C) A native gel was conducted to test the intact nature of the procapsid control without denaturation. Pre- and post-induction samples were used as positive controls for procapsid samples. (D) Samples were run through size exclusion chromatography (SEC) to further confirm procapsid presence. Procapsids are known to contain an elution time of around 20-30 minutes. Peaks present at around 20 minutes indicate the presence of intact procapsids.

λ

targeted drug delivery method by decorating the outside shell with ligands specific to target receptors (Koudelka *et al.* 2015). However, encapsulation of drugs instead of external decoration may prove to be a favorable method of delivery by increasing payload security and volume. Thus, the controlled *in vitro* assembly of bacteriophage λ procapsids as VNPs can aid with this endeavor.

Procapsid shells are constituted of two main proteins: ~ 400 copies of gpE, the major capsid protein, and gpD, the stabilization protein, present in equal ration to gpE. These two proteins arrange to form an icosahedral structure 50-60 nm in diameter (Lander *et al.* 2008). *In vivo* assembly of the capsid head is also initiated by ~70-200 copies of the internal scaffolding protein, gpNu3, as a chaperone for shell formation that is subsequently degraded (Medina *et al.* 2011). Hence, the utilization of these natural capsid protein ratios *in vitro* is theorized to be a promising avenue for fabrication in solution.

In this study, methods of purification and isolation of the capsid proteins gpE, gpD and gpNu3 are evaluated as a precursor to their combination *in vitro.* Previous studies have exhibited limited success in isolated protein purity, which is theorized to be one of the obstacles preventing full icosahedral structure formation. Additionally, through Cryo-EM imaging, former attempts at *in vitro* capsid formation yields abnormal, long, tubular aggregates of λ proteins when utilizing a 1:1:1 gpE:gpD:gpNu3 ratio. Thus, this study also aims to facilitate the refinement of protein ratios to increase intact procapsid yield.

Results

Purification of intact procapsids as a control

In order for later analysis of *in vitro* procapsid assembly, it is necessary to produce fully intact procapsids as a control *in*

vivo. Sucrose gradient purification yields bands that contain these procapsids and lysis residues separated by size. SDS-PAGE results display an intense band at around 39 kDa for the bottom sucrose gradient band, suggesting the presence of gpE. Top and middle band sucrose pulls yielded no bands, suggesting the absence of major capsid proteins (Fig. 1a). Western blot analysis was conducted to further confirm the presence of the major capsid protein, gpE. Chemiluminescent signals were displayed for both of the induction controls, as well as the bottom band of the procapsid sucrose gradient, confirming the presence of gpE (Fig 1b).

To verify the intact nature of these capsid proteins, native gel analysis was conducted without sample denaturation. Positive controls were obtained from the bacterial cell culture pre-induction and post-induction of cell growth. Negative controls were obtained by the denaturation of samples at 70ºC for 10 minutes. Because of the lack of chemiluminescent signal from the previous western blot, top and middle band samples were not loaded onto the native gel for analysis. The bottom band sample displayed an intense band with similar path length to the post-induction positive control, indicating the presence of intact procapsids (Fig 1c).

For further confirmation of procapsid control integrity, samples were analyzed using size exclusion chromatography (SEC). Intact procapsids are known to elute off the column at around 20-30 minutes due to their relatively larger size. Small peaks present at around 40-50 minutes could indicate small protein aggregates or other impurities present after a long, 90-day storage period. However, sharp peaks present at around 20 minutes indicate the presence of intact procapsids for use as a control for the further combination of capsid proteins *in vitro* (Fig 1d).

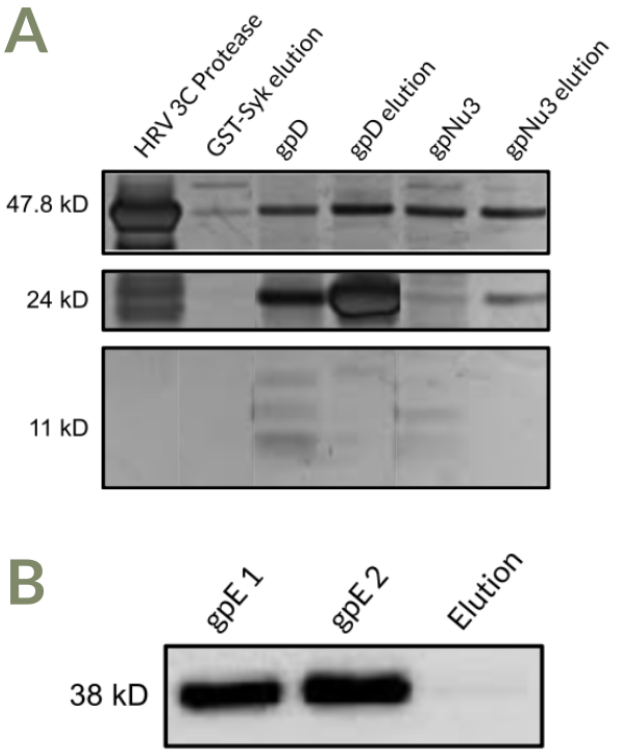

Figure 2. **On-column cleavage and purification of gpE, gpD, and gpNu3 using GST-affinity .** (A) A silver stained SDS-PAGE was conducted to visualize extent of protein purity for gpD and gpNu3 due to lack of specific antibodies. Banding for HRV 3C protease present at all samples and banding for GST present at all samples is indicatory of a lower-than-expected purity sample yield. Bands present at around 11-14 kDa suggests some presence of purified gpD and gpNu3. (B) A western blot was utilized to visualize purified gpE samples. The presence of intense banding at the major capsid protein known kDa of 38.9 suggests the success of the HRV 3C protease cleavage reaction on the gpE samples to detach GST. No banding in the gpE elution sample further proves cleaved gpE purity.

Purification of individual capsid proteins: gpE, gpD, and gpNu3

To examine the success of individual capsid protein purification using glutathione spin-columns, samples were run through SDS-PAGE and western blotting. Due to the lack of antibodies specific to gpD and gpNu3, an SDS-PAGE was conducted using silver stain for small protein visualization. The protease utilized in the GST-cleavage reaction (HRV 3C) is known to have a kDa of around 47.8. The presence of bands at this known molecular weight indicates the presence of protease within all gel samples (Fig 2a).

The glutathione-S-transferase (GST) tags expressed by all recombinant capsid proteins have a molecular weight of around 26 kDa. Bands present at this location in gpD and gpNu3 samples and elution indicates the presence of GST. This implies limited success in obtaining ultra-pure gpD and gpNu3 samples. GST-indicating bands were also present in the GST-syk elution, albeit very faint (Fig 2a).

The molecular weight for gpD and gpNu3 are 11.4 and 13.4 kDa, respectively. Bands present at around 11 kDa in gpD and gpNu3 purified samples in tandem with the absence of banding at this molecular weight in the protein elution indicate the presence of purified recombinant protein without the GST tag, and thus suggest GST cleavage success. Faint banding implies a small protein concentration and can be due to improper loading amounts (Fig 2a).

The molecular weight for gpE is 38.2 kDa. Intense banding present in a western blot at around 38 kDa indicates the presence of purified gpE without the GST-tag attached. The absence of banding in the purified gpE elution sample is

A

Sample #	Ratio (gpE:gpD:gpNu3)	gpE (µL)	gpD (µL)	gpNu3 (µL)	Total volume of protein	Tris Buffer up to 1500 µL	Total sample volume
1	1:1:1	330.000	220.000	291.429	841.429	658.571	1500.000
2	1:0:0.3	330.000	0.000	87.429	417.429	1082.571	1500.000
3	1:1:0.3	330.000	220.000	87.429	637.429	862.571	1500.000

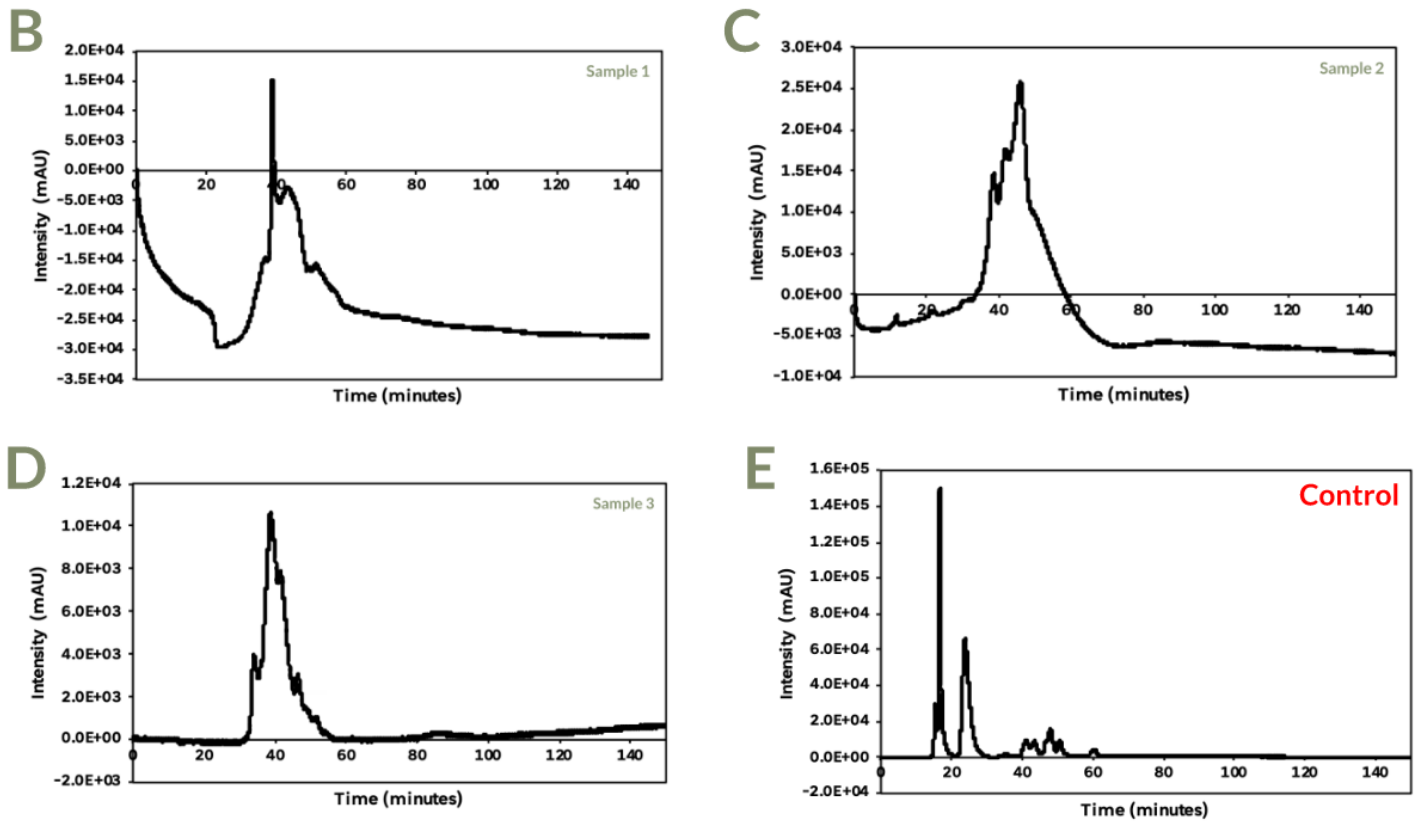

Figure 3. **Smaller capsid protein aggregates are formed *in vitro* .** (A) Three different ratios of gpE:gpD:gpNu3, numbered 1-3, were combined, and analyzed. Volumes of purified protein added to a 2mL reaction vial were calculated and documented in a table using sample concentrations and reference ratios. (B) Incubated samples were analyzed using size exclusion chromatography. Sample 1 yielded an irregular and broad peak at 40 minutes, suggesting smaller protein aggregates. (C) Sample 2 also displayed a broad peak at 40 minutes, reaching a maximum intensity of 2.6 mAU. (D) Sample 3 showed similar results, with a peak at 40 minutes, indicating smaller capsid protein aggregates. Peak sharpness was higher, indicating structure uniformity. (E) SEC data from the procapsid control preparation is shown here as a means of comparison to the *in vitro* combination SEC runs.

evident of higher purity for the major capsid protein samples and indicates the lack of intact gpE-GST after adding HRV 3C protease (Fig 2b). Overall, on-column cleavage using glutathione spin-columns resulted in a lower-than purity yield of recombinant capsid proteins. However, gel banding at molecular weights indicatory of these proteins suggest the presence of cleaved molecules, and thus was utilized in further procapsid *in vitro* assembly with these results in mind.

In vitro assembly of bacteriophage λ procapsids

Volumes of purified capsid proteins samples added to *in* vitro procapsid assembly reaction vials were calculated based on constructed ratios of gpE:gpD:gpnu3 and isolated protein sample starting concentrations. Final calculations were put into a table and numbered 1-3 (Fig 3a).

To test the final extent of procapsid assembly for each ration, samples were analyzed using SEC and compared to data from the procapsid control. Sample 1 (ratio 1:1:1) yielded a broad peak around 40 minutes, suggesting the formation of structures smaller than full icosahedral formations. Maximum intensity reached was around 1.5E4 mAU. Peak broadness can also be indicatory of a wider range of aggregate size, showing the lower uniformity in protein assembly (Fig 3b).

Sample 2 (ratio 1:0:0.3) sees the omission of gpD overall, as well as the decreased concentration of gpNu3 to gpE. This ration yielded a broader peak at around 40 minutes, suggesting the formation of structures smaller than full icosahedral formations. However, maximum intensity reached is higher at around 2.6E4, indicating an increased concentration of capsid protein aggregates at a size that elutes around 40 minutes with a lower concentration of gpNu3 to gpE (Fig 3c).

Sample 3 (ratio 1:1:0.3) adds a proportional concentration of gpD to gpE. Again, a peak was observed at 40 minutes, confirming the presence of smaller capsid protein aggregates than the full icosahedral structure. Maximum intensity reached was lower, at only 1.1E4 mAU. However, the peak is sharper and cleaner, suggesting higher uniformity within capsid protein formation with the addition of the decoration protein, gpD (Fig 3d). Observations and conclusions were made by comparing *in vitro* combination results with the SEC graph of the PT7cap+E procapsid control, seen in figure 3e.

Discussion

Bacteriophage λ procapsids have the potential to be utilized as molecular transporters for drugs to targeted sites within the body. Because of their combinatorial nature of individual capsid proteins that constitute the fully formed icosahedral shell, isolation and combination of these proteins, gpE, gpD, and gpNu3, *in vitro* has the potential to encapsulate drugs of choice. Thus, methods of capsid protein purification were evaluated in this study as the first step in assembly. Additionally, the subsequent procapsid structure viability combining gpE:gpD:gpNu3 in differing concentrations extended insight into *in vitro* procapsid formation . Using mainly size exclusion chromatography (SEC), it was found that a lower concentration of gpNu3 to gpE (0.3:1) yielded increased capsid protein aggregate formation. Furthermore, the addition of gpD at a 1:1 ratio to gpE yielded an increased uniformity in aggregate size. Results during protein purification and after capsid protein combination gave the following insights into the *in vitro* assembly of bacteriophage λ procapsid methodology.

Further purification steps are needed for individual capsid protein preparation

After SDS-PAGE analysis of gpD and gpNu3 protein purification, the presence of GST in the protein samples suggest a lower-than-expected purity sample yield. This suggests one main possibility: protein binding capacity of the GST-affinity resin bed volume was surpassed, thus GST-capsid protein structures could not bind and ended up in the flow through. Further testing of maximum resin binding capacity is needed to decrease GST presence in final protein sample. Additionally, a second size-exclusion purification step after GST-affinity can aid in the increase in purity of the isolated protein samples.

Additionally, HRV 3C protease present in the protein samples also suggested further purification steps are needed to separate capsid proteins from protease residues. Future studies should incorporate another size-exclusion pass through to filter out remaining protease in order to yield gpE, gpD, and gpNu3 with a higher purity rate. The presence of residual GST and protease could have hindered the congregation of capsid protein quaternary structure, and thus will need to be improved in future studies.

In vitro assembly of capsid proteins yield smaller, aberrant structures relative to full, intact procapsids

Using information obtained from previous studies surrounding the structure of bacteriophage λ *in vivo*, ratios of gpE:gpD:gpNu3 were formed accordingly. Sample 1 (see Fig. 3a) was including as a means of replicating results from the Koudelka research lab during Point Loma Nazarene university 2022 Summer Research that were imaged using Cryo-EM at Scripps Research Institute in La Jolla. The 2022 1:1:1 sample revealed long, tubular protein aggregates that were smaller than full icosahedral structures (Fig A1). After analyzing SEC data for the 2023 1:1:1 sample, a broad peak at 40 minutes suggests the formation of similar structures and can be used as a baseline for other samples.

Sample 2 was included as a means of testing the effect of lowering the gpNu3 concentration to the optimal amount stated in the paper by Medina *et al.* (2011). Utilizing the 0.3:1 ratio of gpNu3 to gpE yielded the highest concentration of intact procapsids in the 2011 study, albeit still not with complete purity. In this study, sample 2 did yield

the highest concentration in protein structure formation, which is consistent with the 2011 findings. The peak was also sharper than that of sample 1, which implies increased aggregate size uniformity. However, the peak was observed at 40 minutes, which implies smaller structures that eluted off the column later than the icosahedral capsids observed in the SEC data for the procapsid control (Fig 3 c,e). There are multiple conclusions that can be made here: similar tubular structures were constructed as observed in the 1:1:1 ratio sample, or there was a likely issue with the current recombinant plasmid used for the procapsid control that this data was compared to (PT7cap+E). Cryo-EM images obtained during the previous 2022 Summer Research of the pT7cap+E procapsid controls revealed the presence of gpB, an additional "portal" protein attached to the capsid shell (Fig A2). The addition of this protein allows for the sample to elute off the SEC column at an earlier time due to the larger molecular weight, thus skewing control data to show procapsids coming off at 20-30 minutes. If this is the case, structure formation in sample 2 could be closer in similarity to those findings from the 2011 study by Medina *et al.* (2011).

Sample 3 includes the addition of gpD in direct proportion to the concentration of gpE. In the study by Lambert *et al.* (2016), it was stated that gpD is added in this ratio during natural bacteriophage λ formation *in vivo* in order to combat internal capsid pressure after genome packaging, but it is not entirely necessary for pre-genome immature procapsid formation. Thus, it's necessity in the *in vitro* assembly of procapsids was debated. Slight changes to SEC data results before the addition of gpD (sample 2, see Fig 2c) and after the addition of gpD (sample 3, see Fig 2d) were observed. Lower concentrations of protein aggregates were shown, but a sharper and cleaner peak at 40 minutes also resulted versus the broader peak observed in sample 2. Thus, the addition of gpD suggests its role in the uniformity of structure size and thus cemented it of increased importance to procapsid stability.

However, it should be noted that further analysis should be made in the prediction of capsid protein aggregation structure. One possible route, as previously stated, would be the subsequent step of Cryo-EM. Microscopic sample images contain the information needed to make concrete conclusions of procapsid assembly.

Conclusion and future directions

In sum, this study has given insight in the necessity of improving purification protocol of individual capsid proteins. Additionally, utilizing a lower gpNu3 ratio to gpE and a proportional ratio of gpD to gpE yields promising results into controlling the formation of procapsids *in vitro*. Further tinkering with these ratios, as well as the addition of imaging analysis is a hopeful avenue on the path for the end-goal of using bacteriophage λ as VNPs in a clinical setting for targeted drug delivery.

Using information obtained from this current study, future directions concerning the improvement of the methodology surrounding assembly of bacteriophage λ procapsids *in vitro* were evaluated. One possible route would be the addition of another protein crucial to procapsid formation, gpC, which is the protease involved in the degradation of gpNu3 after capsid formation (Medina *et al.* 2010). Aberrant structures exhibited in the SEC data from this study (see Fig. 3) have implications in being caused by protein residuals and their interference. With the addition of gpC, scaffolding residuals can be disposed of in a process that mirrors the natural procapsid assembly pathway present *in vivo*.

Another potential avenue of study could be the incorporation of a "molecular doorstop". In cellular processes such as ER translocation, membrane channels that allow proteins to cross organelle membranes are plugged with helical secondary structures that inhibit the further passage of molecules (Alberts *et al.* 2008). This mechanism contains the propensity to be applied to structures such as procapsids that contain gpB, the protein that creates a "portal" or "hole" in the final icosahedral structure (Appendix B). By repurposing the transfected *E.coli* utilized as this study's control (PT7cap+E) that manufactures intact procapsids *in vivo*, future studies can essentially fabricate a secondary protein structure that can act as a "plug" that nestles within the procapsid portal complex after concentration-based cargo loading. However, the viability of this mechanism is still in question.

Materials and Methods

Purification of intact procapsids as a control

E. coli transfected with the plasmid pT7cap+E, which expresses the bacteriophage λ capsid proteins gpE and gpD, were grown in a culture overnight at 37ºC in a shaking incubator. Culture media containing 1M ampicillin-treated LB was utilized to select for transfected bacterium. A larger culture containing 1L 2xYT, 15 mL 1M sodium phosphate buffer, 5 mL 1M glucose, and 1 mL 1M ampicillin, was inoculated using the overnight culture. Upon reaching an

absorbance reading of 0.700-0.800 at 600 nm, the culture was induced with IPTG and incubated for 2 more hours.

The culture was aliquoted and spun down at 3,500 rpm at 4ºC for two intervals of 15 minutes. Pellets were subsequently isolated and resuspended in 3 mL aliquots of 0.4% DNase mixed with 20 mL of Tris buffer, pH 7.4, containing 0.1 M NaCl and 0.1 M $MgCl_2$ for cell lysis with sonication (10x10 second intervals). The crude lysate was then spun at 8,000 rpm at 4ºC for 25 minutes. The supernatant was kept and spun at 27,000 rpm at 4ºC for 3 hours, in which the resulting pellet was overlayed with 1 mL of Tris buffer and kept at 4ºC overnight.

The overlay supernatant was then placed over a 10%-40% sucrose gradient in a Beckmann Ultra-Clear polypropylene centrifuge tube and spun at 27,000 rpm at 4ºC for 3 hours. Resulting bands were pulled with 10 mL syringes fixed with 21g needles and kept separated for a second sucrose gradient using the same procedure. The samples were then dialyzed using 15 mL capacity 20,000 MWCO Dialysis Cassettes (Thermo Scientific™) for 3 hours against Tris buffer and concentrated to under 1 mL. Concentrations were obtained using the Thermo Scientific NanoDrop 2000c spectrophotometer and stored at 4ºC for 90 days.

Samples were then analyzed using both western blotting and SDS-PAGE. Primary antibodies (poly anti-rabbit λ-gpE) were obtained from Dr. Kristopher Koudelka (Department of Biology, Point Loma Nazarene University) and HRP-conjugated goat anti-Rabbit IgG secondary antibodies were obtained from Thermo Scientific. They were then utilized for chemiluminescent imaging of the procapsid controls.

Samples were also analyzed concurrently with size exclusion chromatography (SEC) using a Cytiva Superose 6 Increase 10/300 GL attached to a Shimadzu FPLC containing Tris buffer at 0.5 mL min^{-1} for 150 minutes. Peaks were then analyzed, and data was saved for later examination.

Purification of individual capsid proteins: gpE, gpD, and gpNu3

Three strains of *E. coli* transfected with plasmids pGEX-6P-3-"C"-gpE, pGEX-6P-3-"C"-gpNu3, and pGEX-6P-3-"C"-gpD, which all express the individual capsid proteins gpE, gpNu3, and gpD with a glutathione-s-transferase (GST) protein tag attached, were cultured using the same procedure as the intact procapsid control up until sonication. Halt™ protease inhibitor cocktail (100x) was added immediately post-lysis to prevent GST tag auto-cleavage in solution. The crude lysate was spun at 7,300 rpm at 4ºC for 25 minutes, and the supernatant was kept and sterile filtered over a 0.22 µm filter.

GST-affinity protein purification and on-column cleavage was conducted using protocols from the Thermo Scientific 0.2 mL Glutathione Spin Columns in tandem with Pierce™ HRV 3C Protease. A western blot and SDS-PAGE were subsequently conducted to test the extent of GST-gpE protein purification and cleavage, in addition to another SDS-PAGE
to test the extent of gpD and gpNu3-GST.

In vitro assembly of bacteriophage λ procapsids

Various ratios of isolated gpE, gpD, and gpNu3 were combined with enough Tris buffer to reach a 1.5 mL sample volume, then incubated with end-over-end mixing overnight at 4ºC in a 2 mL capacity Eppendorf tube. The samples were then dialyzed using 0.5 mL capacity 20,000 MWCO Dialysis Cassettes (Thermo Scientific) for 3 hours against Tris buffer and concentrated to under 0.5 mL.

Samples were then loaded on a Superose 6 Increase 10/300 GL column equilibrated with Tris buffer at 0.5 mL min^{-1} for 150 minutes. Final conclusions were drawn from peaks present on the resulting chromatographs.

References

Alberts, Bruce *et al. Molecular Biology of the Cell.* New York, NY,Garland Science, 2008.

Anselmo, A.C. and S. Mitragotri. 2016. Nanoparticles in the Clinic. *Bioeng Transl Med.* 1:10-29. doi: 10.1002/btm2.10003.

De Jong, W.H. and P.JA. Borm, 2022. Drug Delivery and nanoparticles: Applications and hazards. *International Journal of Nanomedicine.* 3:2, 133-149, DOI: 10.2147/ijn.s596

Koudelka, K.J., M. Manchester, and N.F. Steinmetz. 2015. Virus-Based Nanoparticles as Versatile Nanomachines. *Annu Rev Virol.* 2(1):379-401. doi: 10.1146/annurev-virology-100114-055141

Lander, G.C., A. Evilevitch, M. Jeembaeva, C.S. Potter, B. Carragher, and J.E. Johnson. 2008. Bacteriophage Lambda Stabilization by Auziliary Protein gpD: Timing, Location, and Mechanism of Attachment Determined by Cryo-EM. *Cell Press.* 16(9):1399-1406. doi.org/10.1016/j.str.2008.05.016

Medina, E.M., B.T. Andrews, E. Nakatani, and C.E. Catalano. 2011. The bacteriophage lambda gpNu3 scaffolding protein is an intrinsically disordered and biologically functional procapsid assembly catalyst. *J Mol Biol.* 412(4): 723-36. doi: 10.1016/j.jmb.2011.07.045

Medina, E.M., D. Wieczorek, E.M. Medina, Q. Yang, M. Feiss, and C.E. Catalano. 2010. Assembly and Maturation of the Bacteriophage Lambda Procapsid: gpC Is the Viral Protease. *J Mol Biol.* 401(5): 813-30. https://doi.org/10.1016/j.jmb.2010.06.060

APPENDIX A

CRYO-EM IMAGES FROM THE 2022 KOUDELKA SUMMER RESEARCH LAB

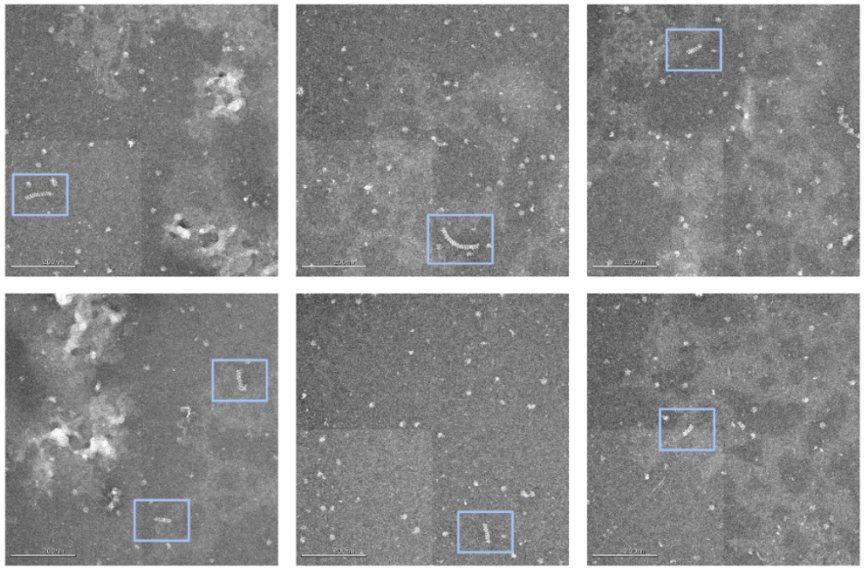

Figure A1. **Long, tubular structures are formed using a 1:1:1 gpE:gpD:gpNu3 ratio *in vitro* .** Combination samples made by the 2022 Koudelka summer research lab at Point Loma Nazarene University were analyzed using Cryo-EM at Scripps Research Institute in La Jolla. A 1:1:1 ratio of capsid proteins yielded aberrant structures that are not full icosahedral formations.

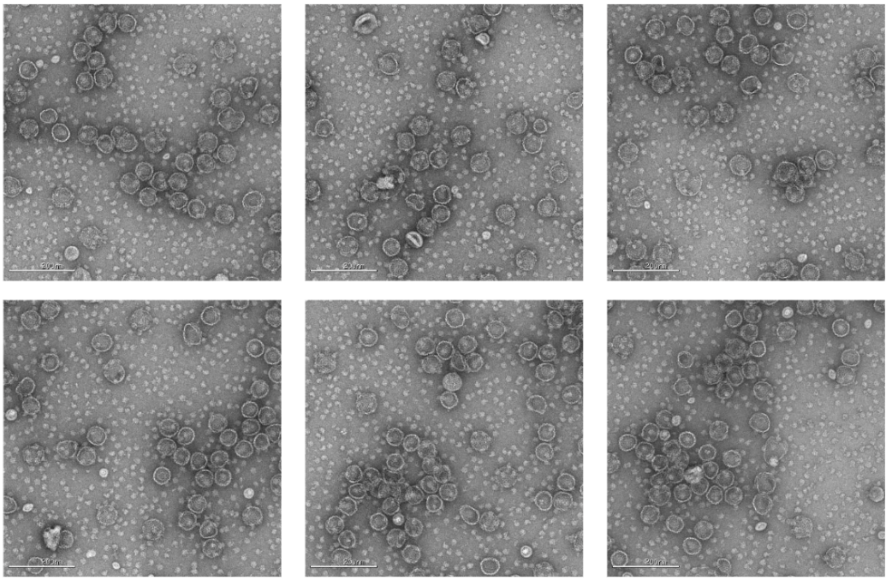

Figure A2. **gpB is present in the PT7cap+E control.** Control samples made by the 2022 Koudelka summer research lab at Point Loma Nazarene University were analyzed using Cryo-EM at Scripps Research Institute in La Jolla. Fully intact icosahedral formations were expected and exhibited. However, the presence of the gpB portal protein was unexpected.

APPENDIX B

DIAGRAM OF PROCAPSID FORMATION

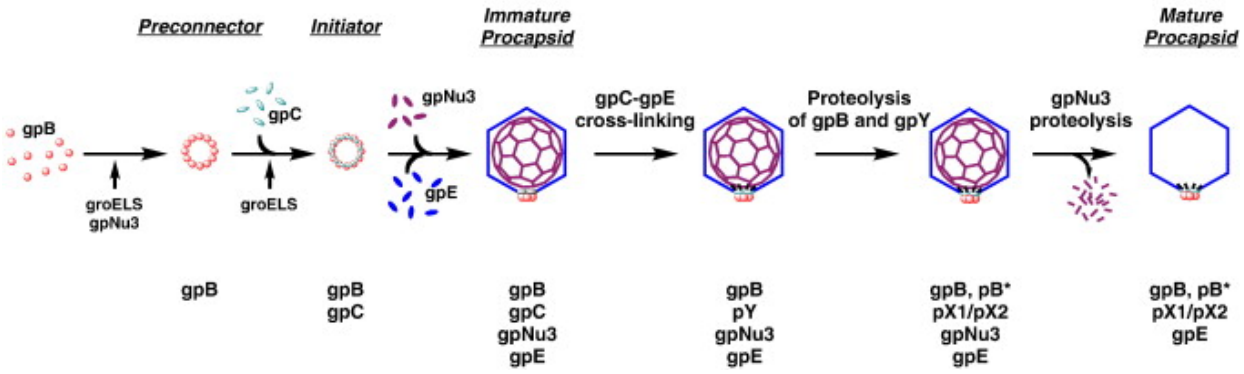

Appendix B. **gpB assembles intro a portal as the initiation step of procapsid formation *in vivo*.** Using information obtained from the paper by Medina *et al.* (2010), a diagram outlining procapsid formation *in vivo* is shown here. The formation of portal initiates the mechanism of capsid maturation, which will later on act as the entrance for internal genome packaging.